Osteoarthritis and Cartilage Open 5 (2023) 100386

Contents lists available at ScienceDirect

Osteoarthritis and Cartilage Open

journal homepage: www.elsevier.com/journals/osteoarthritis-and-cartilage-open/2665-9131

Interleukin-6 receptor blockade improves bone healing following ischemic osteonecrosis in adolescent mice

Gen Kuroyanagi [a,b,1], Nobuhiro Kamiya [a,c,1], Ryosuke Yamaguchi [a,d], Harry K.W. Kim [a,e,*]

[a] Center for Excellence in Hip, Scottish Rite for Children, Dallas, TX 75219, USA
[b] Department of Orthopedic Surgery, Nagoya City University Graduate School of Medical Sciences, Nagoya, Aichi 467-8601, Japan
[c] Faculty of Budo and Sport Studies, Tenri University, Nara 6320071, Japan
[d] Department of Orthopaedic Surgery, Graduate School of Medical Sciences, Kyushu University, Fukuoka 812-8582, Japan
[e] Department of Orthopaedic Surgery, University of Texas Southwestern Medical Center, Dallas, TX 75390-8883, USA

ARTICLE INFO

Handling Editor: Professor H Madry

Keywords:
Adolescent ischemic osteonecrosis
IL-6 receptor blockade
Legg-Calve-Perthes disease
Animal model
Cartilage
VEGF

ABSTRACT

Objective: Juvenile ischemic osteonecrosis (JIO) of the femoral head is one of the most serious hip disorders causing a permanent deformity of the femoral head in childhood. We recently reported that interleukin 6 (IL-6) is significantly increased in the hip synovial fluid of patients with JIO and that articular chondrocytes are primary source of IL-6. Adolescent JIO is particularly challenging to treat and has poor outcome. This study determined if IL-6 receptor blockade prevents bone loss and improves the bone healing in adolescent JIO.

Method: Adolescent mice (12-week-old) surgically induced with JIO were treated with either saline or MR16-1, an IL-6 receptor blocker.

Results: Micro-CT assessment showed significantly increased bone volume ($p < 0.001$, Cohen's $d = 2.0$) and trabecular bone thickness ($p < 0.001$, $d = 2.3$) after the MR16-1 treatment. Histomorphometric assessment showed significantly increased osteoblast number ($p < 0.01$, $d = 2.3$), bone formation rate ($p < 0.01$, $d = 4.3$), and mineral apposition rate ($p < 0.01$, $d = 4.1$) after the MR16-1 treatment. The number of osteoclasts was unchanged. Histologic assessment showed significantly increased revascularization ($p < 0.01$) and restoration of the necrotic marrow with new hematopoietic bone marrow ($p < 0.01$). Vascular endothelial growth factor (VEGF) expression was increased in the revascularized area and the articular cartilage, and in the cultured chondrocytes treated with IL-6 receptor inhibitor.

Conclusion: IL-6 blockade in adolescent mice with JIO enhanced bone formation and revascularization. The findings suggest IL-6 receptor blocker as a potential medical therapy for adolescent JIO.

1. Introduction

Legg-Calve-Perthes disease (LCPD) is an idiopathic juvenile ischemic osteonecrosis (JIO) of the femoral head. The age at onset of LCPD is one of the most important prognostic factors of clinical outcome. The onset of LCPD before six years of age is generally associated with a good outcome even without treatment, while age at onset after age nine, and especially in teenagers, is associated with worse outcome [1–3]. Thus, it is established that the onset of JIO at adolescence is challenging to treat and difficult to obtain good clinical results [3,4]. In adolescent JIO, the repair process is significantly impaired with slow revascularization and new bone formation following resorption of the necrotic bone. The impaired healing often results in development of a permanent femoral head deformity, early osteoarthritis, and severe disability [3–6].

Interleukin-6 (IL-6) is emerging as an important pro-inflammatory cytokine in ischemic osteonecrosis (ON). Patients with LCPD showed a significant elevation of IL-6 levels in the synovial fluid of the affected hip, which was 20 times greater than that of the controls [7]. In porcine and murine models of JIO, the induction of ischemic osteonecrosis also produced high levels of IL-6 protein in the synovial fluid as well as *IL-6* gene expression in the articular cartilage and the synovium [8–11]. IL-6 can bind to a soluble (sIL-6R) or membrane-bound IL-6 receptor (mIL-6R), and then associates with two molecules of the transmembrane gp130. This leads to intracellular signal transduction such as the Janus kinase/STAT

* Corresponding author. Scottish Rite for Children, Dallas, TX 2222 Welborn Street, Dallas, TX 75219, USA.
E-mail addresses: kokuryugen@yahoo.co.jp (G. Kuroyanagi), nkamiya1@sta.tenri-u.ac.jp (N. Kamiya), yamaryo@ortho.med.kyushu-u.ac.jp (R. Yamaguchi), Harry.Kim@tsrh.org (H.K.W. Kim).
[1] Both authors equally contributed to this study.

https://doi.org/10.1016/j.ocarto.2023.100386
Received 19 October 2022; Accepted 13 July 2023

pathways [12]. MR16-1, a monoclonal anti-mouse IL-6 receptor antibody, binds both types of IL-6Rs and inhibits IL-6 signaling [13]. The IL-6 signal is transmitted via two different mechanisms, classic and *trans*-signaling. In IL-6 classic signaling, IL-6 binds to mIL-6R, and induces gp130 homodimerization. In contrast, in IL-6 *trans*-signaling, sIL-6R forms complexes with IL-6, and subsequently activate the gp130 signaling pathway in cells that express gp130 but not IL-6R [12]. It has been reported that the inhibition of IL-6 *trans*-signaling prevents increased osteoclasts and trabecular bone loss in an ovariectomized mouse model of osteoporosis [14].

In bone metabolism, IL-6 stimulates osteoclast formation and bone resorption but inhibits bone formation *in vitro* [15,16]. In the IL-6 transgenic mice, which systemically expresses high IL-6 levels, a decreased bone volume was observed due to increased bone resorption and decreased bone formation [17]. In the IL-6 knockout (KO) mice, when we induced ischemic ON, both revascularization and new bone formation are stimulated, concomitant with an increase in the VEGF expression [9]. When ischemic ON was induced in wild-type immature mice (6-week-old) and tocilizumab, an IL-6 receptor blocker, was administrated systemically for 6 weeks, we found preservation of the articular cartilage and the improvement of bone healing [10].

Currently, there is no medical therapy for JIO. Adolescent JIO is challenging to treat due to a lack of effective treatment options and poor outcomes [3,4]. The effects of IL-6 receptor blockade therapy on adolescent JIO have not been investigated. The purpose of this study was to determine if IL-6 receptor blockade prevents bone resorption and improves the bone healing process in adolescent JIO. For this purpose, we treated adolescent mice (12-week-old males) with a monoclonal anti-mouse IL-6 receptor antibody, MR16-1, that has been used in preclinical mouse studies to block the IL-6 binding to its receptor [13,18]. We did not use tocilizumab, a recombinant humanized anti-IL-6R monoclonal antibody, as it neither binds to the mouse IL-6R nor blocks the IL-6 signaling via the mouse IL-6R, because the IL-6R is not conserved between human and mouse.

2. Materials and methods

2.1. Adolescent JIO mouse model

The animal protocols were approved by IACUC of the University of Texas Southwestern Medical Center. Clinically, LCPD is 4–5 times more common in males than females, thereby we focused on males in this study. A total of 53C57BL6/J wild-type male mice at 12 weeks of age (Jackson Laboratory, Bar Harbor, ME), which is skeletally immature, adolescent age based on mouse growth curve and bone strength [19–21], were randomly assigned into the saline group (n = 25) or the MR16-1 group (n = 28) (Table 1). The sample size was calculated to obtain 80% power with alpha = 0.05 and large effect-size (i.e., Cohen's $d >$ 0.8–0.9) based on our previous study [10]. JIO was surgically induced on the distal femoral epiphysis under isoflurane anesthesia, as previously described [22,23]; this model produced almost 100% ON in immature [22] and adolescent mice [23]. Briefly, the blood vessels supplying the right distal femoral epiphysis (i.e., a branch of the popliteal vessel and branches of the medial, central, and lateral genicular vessels) were identified and cauterized. We used the un-operated left side as an internal, contralateral control instead of sham-operated mice in this study. This is based on our previous study which showed no significant difference between the internal, contralateral controls compared to the sham-operated controls in terms of their TUNEL staining and micro-CT analysis of trabecular bone morphology including trabecular bone volume percent (BV/TV), trabecular bone thickness (Tb.Th), trabecular bone number (Tb.N), and trabecular separation (Tb.Sp) [22].

Table 1
Number of mice analyzed.

Mouse group by treatment and post-surgical week	*Saline 2 weeks*	*MR16-1 2 weeks*	*Saline 4 weeks*	*MR16-1 4 weeks*
Total number of mice operated	7	8	18	20
Micro-CT trabecular bone analysis			15	15
H&E, Revascularization	7	8	13	15
N.Ob/BS, N.Ob/TA			8	8
TRAP, N.Oc/BS, N.Oc/TA			8	8
Fluorochrome double labeling			5	5
VEGF staining	7	8		

Mice were randomly assigned into the MR16-1 group (n = 28) or the saline group (n = 25). Mice were sacrificed at post-surgery 2 weeks (n = 15) or 4 weeks (n = 38).

For postoperative pain management, buprenorphine HCL (0.05 mg/kg) was administrated subcutaneously once pre-operatively and every 8–12 h for 48 h post-operatively. Mice were euthanized by CO_2 asphyxiation followed by cervical dislocation. Mice were euthanized by CO_2 asphyxiation followed by cervical dislocation.

2.2. Administration of MR16-1 into an adolescent JIO mouse model

The anti-mouse IL-6 receptor neutralizing antibody MR16-1 (0.5 mg/animal, Roche Chugai, Tokyo, Japan) [13,18], or saline was intraperitoneally administrated. The mice received injections 3 times per week for 2 or 4 weeks from the day of surgery until euthanasia [2 weeks (saline; n = 7, MR16-1; n = 8), 4 weeks (saline; n = 18, MR16-1; n = 20)] (Table 1).

2.3. Micro-CT analysis of distal femoral epiphysis

The distal femoral epiphyses were imaged with a micro-CT scanner (SKYSCAN1172, Aartselaar, Belgium, 8 μm thickness, 50 kV of energy, and 200 mA of intensity) [9,10,22]. BV/TV, Tb.Th, Tb.N, and Tb.Sp were obtained after excluding cortical bones. All coronal images from each femoral epiphysis were analyzed in a blinded manner (n = 15 per group at 4 weeks) (Table 1).

2.4. Histological analysis

The distal femoral epiphyses were fixed with 10% formalin, decalcified in 10% EDTA for 5 days, embedded in paraffin, cut into 5 μm sections, and stained [9,22,23]. H&E staining was performed according to a standard protocol [2 weeks (saline; n = 7, MR16-1; n = 8), 4 weeks (saline; n = 13, MR16-1; n = 15)] (Table 1). Osteoblasts were identified as cuboidal cells attached to the bone surface (n = 8 per group at 4 weeks) (Table 1). As previously described [24], tartrate-resistant acid phosphatase (TRAP) and von Kossa and McNeal tetrachrome staining were performed to determine the osteoclast number (n = 8 per group at 4 weeks) (Table 1).

The area of revascularization and replacement of the necrotic bone marrow by new hematopoietic marrow was determined on H&E-stained sections using the Image J software. The area of revascularization was defined as the area where necrotic marrow is replaced by invading vascular tissue or new hematopoietic bone marrow. The measurements were performed by an independent observer blinded to the groups [2 weeks (saline; n = 7, MR16-1; n = 8), 4 weeks (saline; n = 13, MR16-1; n = 15)] (Table 1).

For immunohistochemistry, a mouse polyclonal antibody against VEGF or IL-6 (Abcam, Cambridge, MA) was used as the primary antibody, followed by a secondary antibody. The staining was visualized with 3,3′-diaminobenzidine tetrahydrochloride (Sigma-Aldrich, St. Louis, MO). Mouse IgG was used as isotype controls.

2.5. Fluorochrome labeling analysis by dynamic bone histomorphometry

Calcein (0.01 mg/g body weight) and xylenol orange (0.09 mg/g body weight) were administered intraperitoneally on day 7 and day 2 prior to euthanasia, respectively [23] (n = 5 per group at 4 weeks) (Table 1). Five-micron thick undecalcified MMA sections were prepared

and assessed under a fluorescent microscope. The dynamic bone formation parameters including bone formation rate per bone surface (BFR) and mineral apposition rate (MAR) were determined in 3 sections per distal femoral epiphysis using Bioquant Osteoimager software (Bioquant Image Analysis Corp., Nashville, TN), as previously described [9].

2.6. Human primary cell culture and tocilizumab addition

Primary chondrocytes were isolated from human articular cartilage (IRB protocol Study ID: STU012011-114) [25] and were pretreated with tocilizumab, a humanized anti-interleukin-6 receptor antibody as an analog of MR16-1, at either 1 μg/ml or 10 μg/ml concentration for 1 h, followed by interleukin-1β (recombinant human IL1-β; 12.5 ng/ml, R&D systems, Minneapolis, MN, USA) treatment to stimulate IL-6 [26] under normoxia (20% oxygen) or hypoxia (1% oxygen) for 16 h.

2.7. RNA isolation and real-time RT-PCR

RNA isolation and RT-PCR were performed [10]. PCR reactions, data quantification, and analysis were performed following TaqMan gene expression assays (ABI PRISM 7500, Applied Biosystems, Rotkreuz, Switzerland). Predesigned primers for pro-angiogenic factors including VEGF (Hs00900055_m1), IL-8 (Hs00174103_m1), and tumor necrosis factor alpha (TNF-α: Mm00443260_g1) were used. The target quantity, normalized to an endogenous HSP90 expression, was analyzed in triplicate using the $2^{-\Delta\Delta C(t)}$ method [27].

2.8. Statistical analysis

SPSS software (Ver. 25, IBM, Armonk, NY) was used. Continuous variables and normality were assessed by the Shapiro-Wilk test ($p > 0.05$) and Levene homogeneity variance test ($p > 0.05$). For data with normal distribution and equal variance, paired *t*-test was used for the comparison of ON side vs. control side within treatment group, and unpaired *t*-test was used to compare differences from ON side to control side between MR16-1 group vs. saline group. For data with non-normal distribution, nonparametric tests were used. Wilcoxon rank sum test was used for the comparison of two groups. Kruskal-Wallis test, followed by Mann-Whitney *U* test, was used for the comparison of more than two groups. The mean differences between two groups were expressed with 95% confidence intervals (CIs). Data were expressed by the mean ± standard deviation (SD) or by a box plot with interquartile range, median, and each point. A *p*-value of <0.05 was considered statistically significant. Effect size was determined using Cohen's *d* method [28], which is probably the most commonly used in the literatures of medical science [28], and $d > 0.8$ indicates a large effect size.

3. Results

3.1. IL-6 receptor blockade increased epiphyseal bone volume in adolescent JIO

The micro-CT analysis of distal femoral epiphysis at 4 weeks post-surgery was performed with reconstructed images (Fig. 1A) and

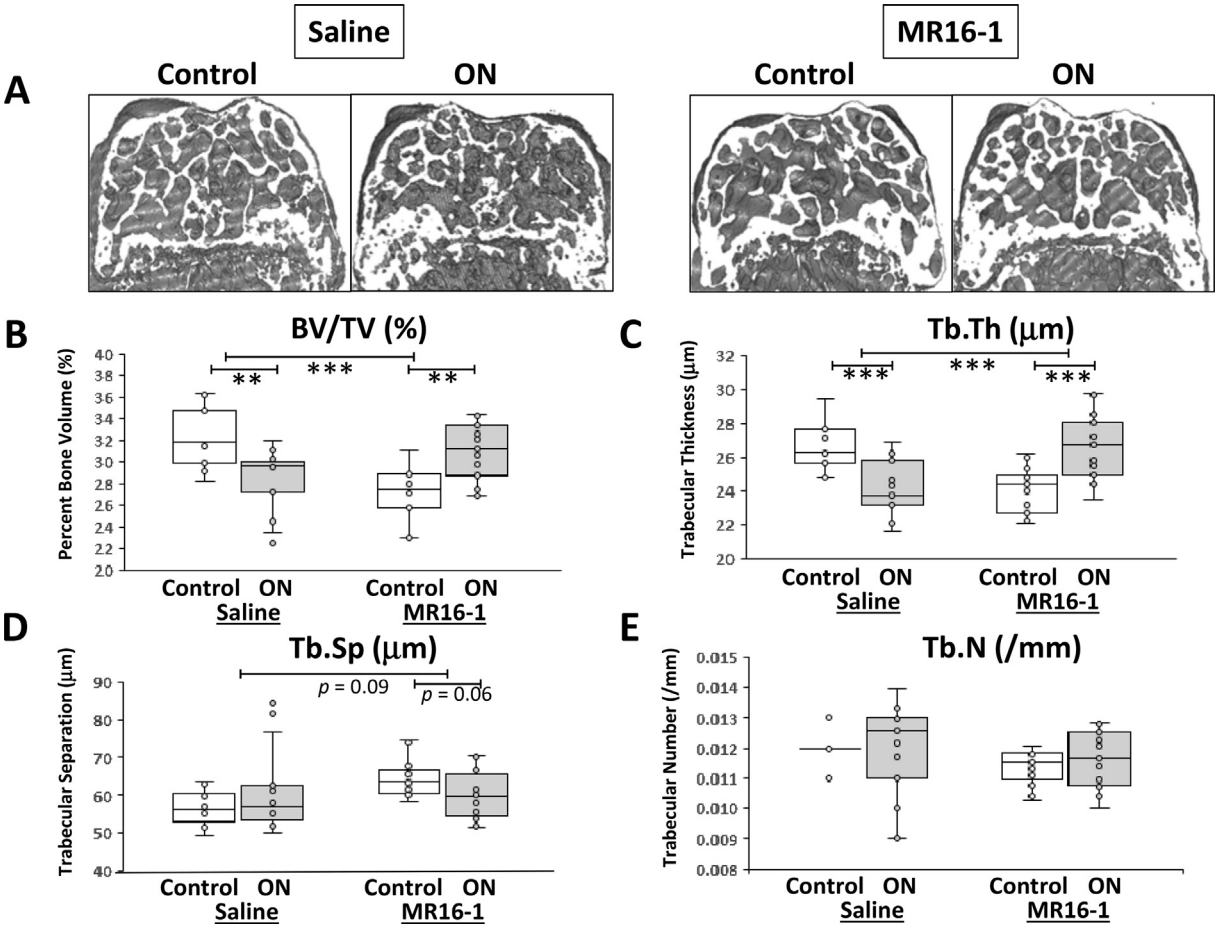

Fig. 1. The micro-CT analysis of distal femoral epiphysis at 4 weeks post-surgery. (A) Representative mid-coronal micro-CT images from the saline and the MR16-1 group. (B) Bar graph of trabecular bone volume (BV/TV), (C) trabecular thickness (Tb.Th), (D) trabecular number (Tb.N), and (E) trabecular separation (Tb.Sp) were assessed by micro-CT. Paired Student's *t*-test or Mann-Whitney *U* test was used for the paired comparison within treatment (i.e., ON side vs. control side). Wilcoxon rank sum test was used for the comparison of differences from the ON side to the control side between treatments (i.e., MR16-1 group vs. saline group). Values were expressed by a box plot. n = 15 per group, $^{**}p < 0.01$, $^{***}p < 0.001$.

morphometric measurements (Fig. 1B–E). In the saline-treated ON side, the trabecular bone volume (BV/TV) was reduced compared to its control while BV/TV was increased in the MR16-1-treated ON side (Fig. 1A and B). The mean difference in the MR16-1 group was significantly higher than that in the saline group (MR16-1 mean difference 3.6 [95% CI: 1.6 to 5.6], saline mean difference −3.3 [95% CI: −5.3 to −1.4], $p < 0.001$, Cohen's $d = 1.97$) (Fig. 1B, Table 1). For trabecular bone thickness (Tb.Th), the mean of saline-treated ON side was significantly reduced compared to its control while the mean of MR16-1-treated side was significantly increased compared to its control. A significant difference was also observed between groups (MR16-1 mean difference 2.6 [95% CI: 1.4 to 3.8], saline mean difference −2.5 [95% CI: −3.6 to −1.3], $p < 0.001$, Cohen's $d = 2.34$) (Fig. 1C). For trabecular bone separation (Tb.Sp), the mean of MR16-1-treated side was insignificantly increased compared to its control ($p = 0.06$) while there was no significant difference between groups ($p = 0.09$, Cohen's $d = 0.86$) (Fig. 1D). For trabecular bone number (Tb.N), no significant difference was obtained (Fig. 1E).

3.2. IL-6 receptor blockade increased bone formation in adolescent JIO

The static histomorphometric analysis of McNeal tetrachrome/von Kossa staining at 4 weeks post-surgery was performed with images (Fig. 2A) and osteoblast parameters (Fig. 2B and C). The images showed increased number of osteoblasts in the MR16-1-treated ON side compared to the saline-treated ON side (Fig. 2A). For osteoblasts per bone surface (N.Ob/BS) and osteoblasts per tissue area (N.Ob/TA), the mean of saline-treated ON side was significantly reduced compared to its control ($p = 0.003$, $p = 0.0006$, respectively) while the mean of MR16-1-treated side was significantly increased compared to its control ($p = 0.015$, $p = 0.014$, respectively). A significant difference was also observed between groups (N.Ob/BS:MR16-1 mean difference 5.2 [95% CI: 1.3 to 9.1], saline mean difference −5.0 [95% CI: −7.8 to −2.3], $p = 0.001$, Cohen's $d = 2.26$ (Fig. 2B, Table 1), (N.Ob/TA:MR16-1 mean difference 66.9 [95% CI: 17.4 to 116.4], saline mean difference −52.0 [95% CI: −73.0 to −31.0], $p = 0.003$, Cohen's $d = 2.28$ (Fig. 2C, Table 1).

The dynamic histomorphometric analysis of calcein and xylenol-orange fluorochrome labeling at 4 weeks post-surgery was performed with images (Fig. 3A) and parameters for new bone formation (Fig. 3B and C). For bone formation rate per bone surface (BFR/BS) and mineral apposition rate (MAR), the mean of saline-treated ON side was significantly reduced compared to its control ($p = 0.008$, $p = 0.013$, respectively) while the mean of MR16-1-treated side was significantly increased compared to its control ($p = 0.005$, $p = 0.006$, respectively). A significant difference was also observed between groups (BFR/BS:MR16-

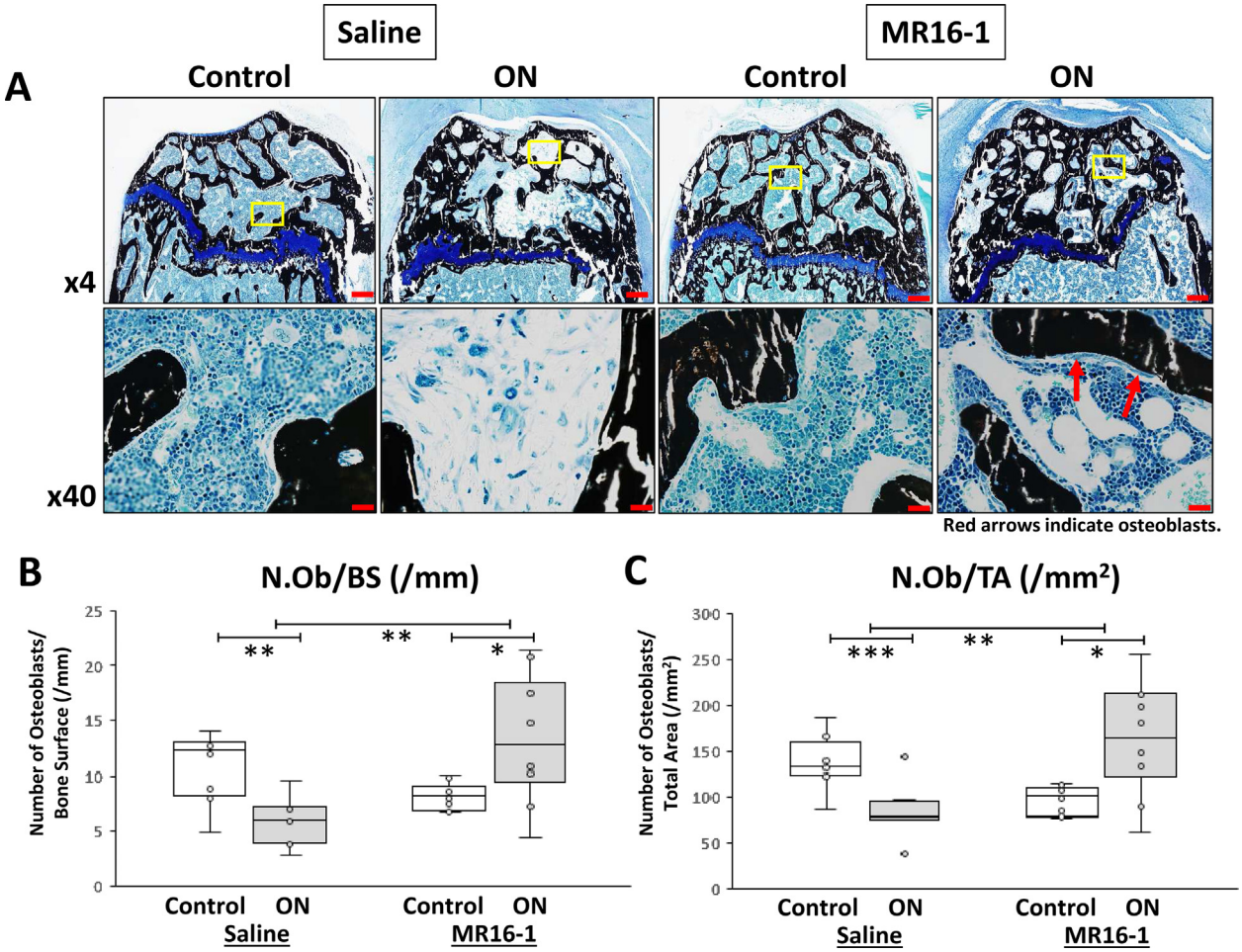

Fig. 2. The static histomorphometric analysis of McNeal tetrachrome/von Kossa staining at 4 weeks post-surgery. (A) Microscopic assessment showed increased presence of osteoblasts on the trabecular surface in the MR16-1 group. Red arrows indicate osteoblasts. The MR16-1-treated ON side had increased restoration of the hematopoietic marrow compared to the saline-treated ON side. The lower panels (40x images) represent the rectangular areas shown in the upper panels (4x images). Scale bars; 200 μm (4x), 20 μm (40x). (B) Static bone histomorphometric analysis showed significant decrease in osteoblast numbers (N.Ob/BS and N.Ob/TA) in the saline-treated ON side compared to its control, whereas these numbers were significantly increase in the MR16-1-treated ON side compared to its control. There were significant differences between treatments (i.e., MR16-1 group vs. saline group). Mann-Whitney *U* test was used within treatment and Wilcoxon rank sum test was used between treatments. Values were expressed by a box plot. n = 8 per group, $^{*}p < 0.05$, $^{**}p < 0.01$, $^{***}p < 0.001$.

1 mean difference 0.39 [95% CI: 0.20 to 0.58], saline mean difference −0.08 [95% CI: −0.13 to −0.04], $p = 0.009$, Cohen's $d = 4.30$ (Fig. 3B, Table 1), (MAR:MR16-1 mean difference 0.99 [95% CI: 0.47 to 1.51], saline mean difference −0.30 [95% CI: −0.49 to −0.11], $p = 0.009$, Cohen's $d = 4.07$ (Fig. 3C, Table 1).

3.3. IL-6 receptor blockade did not alter bone resorption in adolescent JIO

The static histomorphometric analysis of TRAP staining at 4 weeks post-surgery was performed with images (Fig. 4A) and osteoblast parameters (Fig. 4B and C). For osteoclasts per bone surface (N.Oc/BS) and osteoclasts per tissue area (N.Oc/TA), the mean of saline-treated ON side was significantly reduced compared to its control ($p = 0.003$, $p = 0.015$, respectively) while the mean of MR16-1-treated side was unchanged, resulting in no significant difference between groups.

3.4. IL-6 receptor blockade increased revascularization and replacement of the necrotic marrow in adolescent JIO

The assessment of revascularization and new bone formation at 2- and 4-weeks post-surgery were performed with histological images and quantification (Fig. 5A–F). Some necrotic marrow areas were revascularized and replaced by new hematopoietic bone marrow in the MR16-1 group at 2 weeks (Fig. 5A), followed by a greater degree of revascularization and restoration of the hematopoietic bone marrow at 4 weeks (Fig. 5D). The mean percentage of revascularized area in the necrotic epiphysis was significantly higher in the MR16-1 group compared to the saline group at 2 weeks (mean difference 58.9 [95% CI: 26.8 to 90.9], $p = 0.007$, Cohen's $d = 2.1$) (Fig. 5B, Table 1), whereas the restoration of the necrotic marrow with new hematopoietic bone marrow in the MR16-1 group was unchanged compared to the saline group ($d = 1.36$) (Fig. 5C, Table 1). The MR16-1 group, however, had significant higher mean percentage of revascularized area (mean difference 21.1 [95% CI: 6.1 to 36.0], $p = 0.0025$, Cohen's $d = 1.06$) and the restoration of the hematopoietic bone marrow compared the saline group at 4 weeks post-surgery (mean difference 48.1 [95% CI: 23.2 to 72.9], $p = 0.0013$, Cohen's $d = 1.53$) (Fig. 5E and F, Table 1).

3.5. IL-6 receptor blockade increased VEGF expression

VEGF expression was investigated at 2 weeks post-surgery *in vivo* and under hypoxic condition *in vitro*. VEGF immunohistochemistry demonstrated regional increase in the VEGF expression in the areas of repair following the induction of ON in the MR16-1 group compared to the

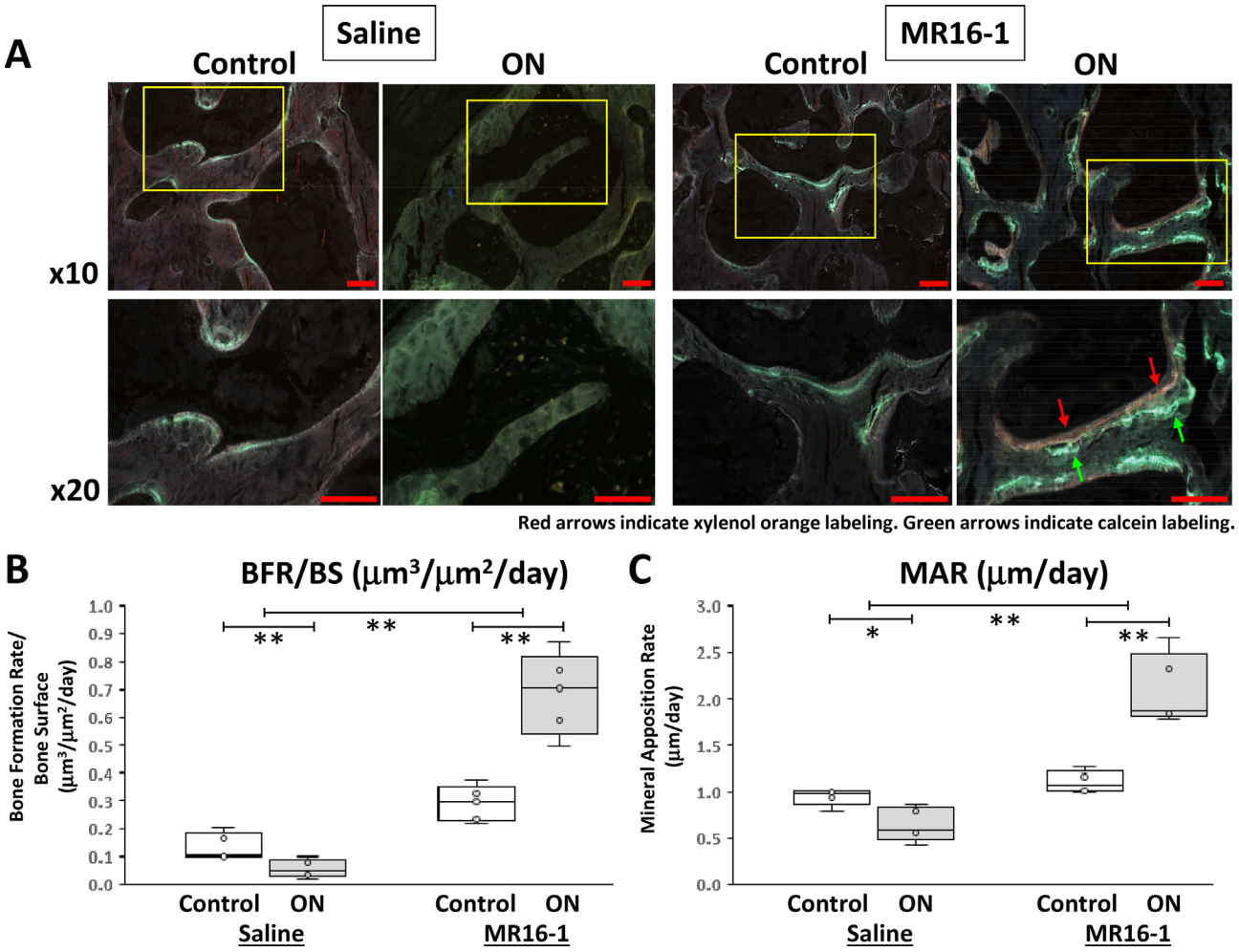

Fig. 3. The dynamic histomorphometric analysis of fluorochrome labeling at 4 weeks post-surgery. (A) The distance between the green (calcein) and orange (xylenol-orange) lines indicates dynamic bone formation for 5 days, which was greater in the MR-16-1 treated ON side compared to the saline-treated ON side. The lower panels (20x images) represent the rectangular areas shown in the upper panels (10x images). Green arrows indicate calcein labeling and red arrows indicate xylenol orange labeling. Scale bars; 50 μm (10x), (20x). (B) The BFR/BS and MAR were decreased in the saline-treated ON side compared to its control, whereas they were increased in the MR16-1-tretaed ON side compared to its control. There were significant differences between treatments (i.e., MR16-1 group vs. saline group). Mann-Whitney *U* test was used within treatment and Wilcoxon rank sum test was used between treatments. Values were expressed by a box plot. n = 5 per group, $*p < 0.05$, $**p < 0.01$.

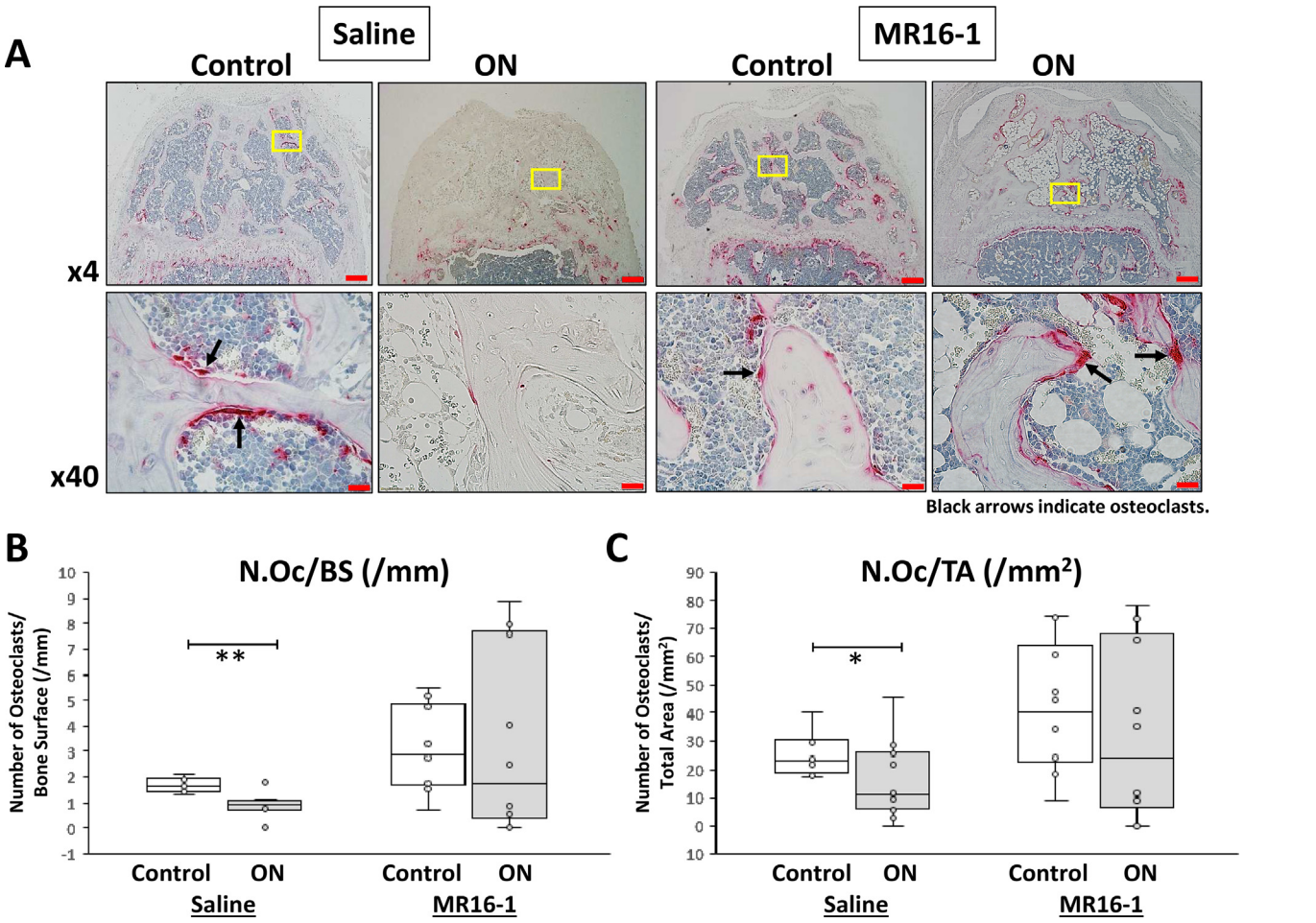

Fig. 4. The static histomorphometric analysis of TRAP staining at 4 weeks post-surgery. (A) The MR16-1-treated ON side had a greater number of osteoclasts compared to the saline-treated ON side. The lower panels (40x images) represent the rectangular areas shown in the upper panels (4x images). Black arrows indicate TRAP positive osteoclasts. Scale bars; 200 μm (4x), 20 μm (40x). (B) The N.Oc/BS and N.Oc/TA were decreased in the saline-treated ON side compared to its control. These numbers in the MR16-1 group were higher than those in the saline groups, however, no difference was observed between the MR16-1-treated ON side and its control side. There was no difference between treatments. Mann-Whitney *U* test was used within treatment and Wilcoxon rank sum test was used between treatments. Values were expressed by a box plot. n = 8 per group, $*p < 0.05$, $**p < 0.01$.

saline group (Fig. 6A). The VEGF expression was enhanced in the articular cartilage in the MR16-1 group compared to the saline group while it was unchanged in the growth plate cartilage (Fig. 6A). The increase in *VEGF* expression in human chondrocytes following IL-6 blockade was reproduced under hypoxia (IL-1 vs. IL-1+1 μg/ml tocilizumab; mean difference 10.7 [95% CI: 8.5 to 12.9], $p = 0.0022$, Cohen's $d = 21.2$, IL-1 vs. IL-1+10 μg/ml tocilizumab; mean difference 12.3 [95% CI: 10.1 to 14.4], $p = 0.0017$, Cohen's $d = 24.2$) (Fig. 6B).

4. Discussion

4.1. Overall findings

This study was stimulated by recent clinical findings of chronic hip synovitis in JIO patients and a significant elevation of IL-6 in their synovial fluid [7]. Because IL-6 is a pro-inflammatory cytokine known to increase bone resorption and decrease bone formation [15,16], we hypothesized that IL-6 elevation plays a pathological role in increasing bone resorption and decreasing new bone formation in JIO. Current study showed that IL-6 receptor blockade significantly increased epiphyseal bone mass (BV/TV) presumably due to enhanced revascularization and replacement of the necrotic marrow with new hematopoietic marrow followed by increase in osteoblast number (N.Ob/BS and N.Ob/TA) and new bone formation (BFR/BS and MAR). IL-6 receptor blockade, however, did not alter osteoclast number. In our previous study we observed a large effect size of tocilizumab on epiphyseal bone mass in immature mice (6-week-old) following JIO based on micro-CT results (BV/TV; Cohen's $d = 1.18$ [10]), however, histomorphometric analysis was not done. In the current study, we also found a large effect size (Cohen's $d > 2$) in the MR16-1-treated adolescent JIO mice (12-week-old) based on micro-CT and histomorphometric results (Supple. Table 1). Taken together, these findings show the therapeutic effects of IL-6 receptor blockade on bone mass in a mouse model of JIO.

4.2. Effects of IL-6 receptor blockade on bone formation

It is known that the effects of IL-6 on osteoblastic activity and bone formation can be different between physiological and pathological conditions [29,30]. In physiological conditions, IL-6 expression levels are very low and IL-6 KO mice do not show alteration of trabecular bone mass as well as osteoblast number [31], indicating negligible role of IL-6 in normal physiological setting. However, under pathological condition, IL-6 may have a different role in new bone formation. In fact, adolescent IL-6 KO mice revealed increased new bone formation following ischemic ON, as assessed by micro-CT and bone histomorphometry [9].

In the current study, we found increased IL-6 immunostaining in the repair tissue invading the necrotic marrow space (Supple. Fig. 1), where bone volume and new bone formation were decreased following

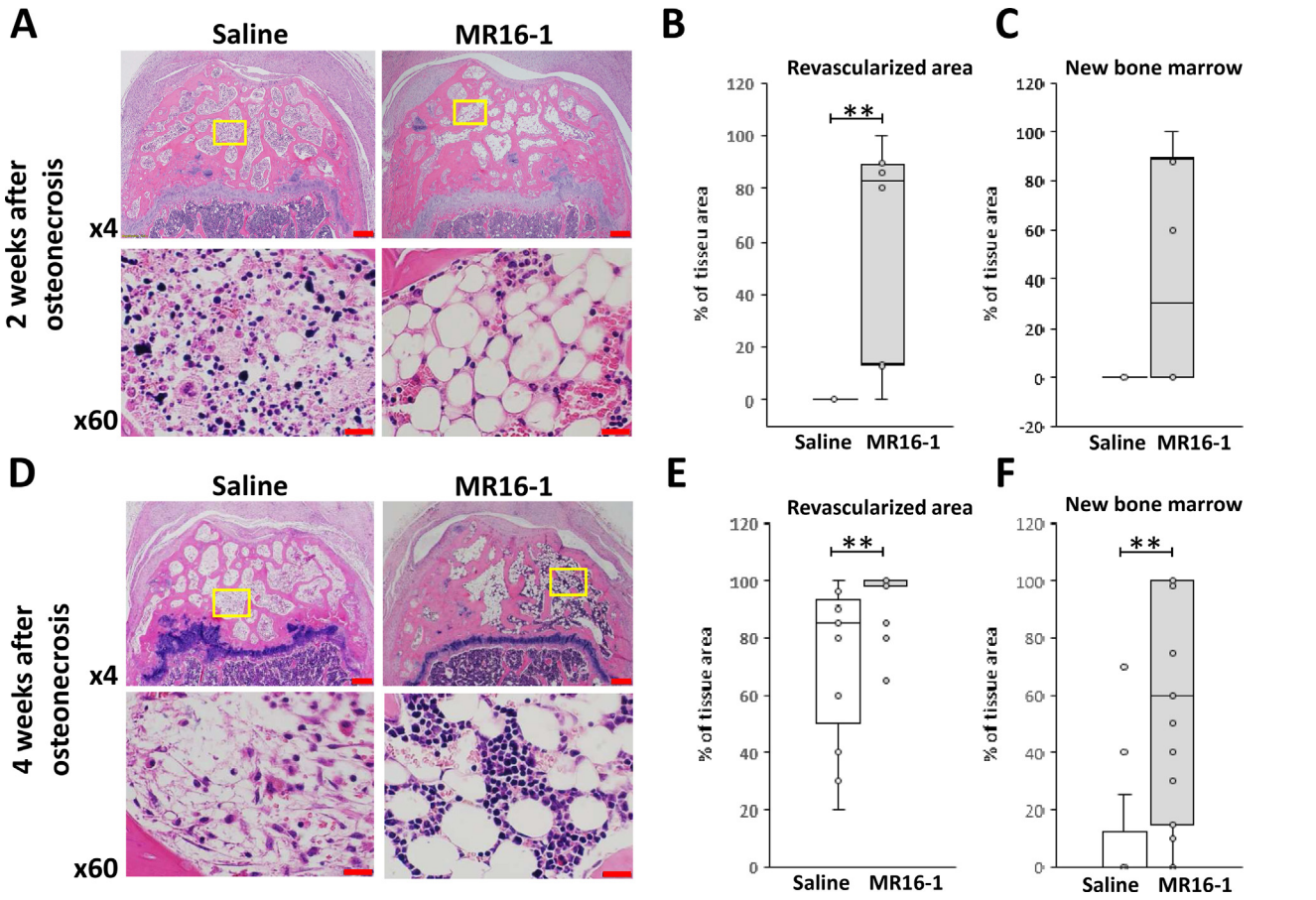

Fig. 5. The assessment of revascularization and new bone formation at 2- and 4-weeks post-surgery. (A, D) Photomicrographs of H&E-stained sections showed increase in revascularization and restoration of the necrotic marrow with new hematopoietic/fatty marrow in the MR16-1 group at 2 weeks post-surgery, which was more evident at 4 weeks post-surgery. The lower panels (60x images) represent the rectangular areas shown in the upper panels (4x images). Scale bars; 200 μm (4x), 20 μm (60x). (B, C, E, F) The quantitative assessment showed the percentage of revascularization and the percentage of replacement of necrotic marrow by new hematopoietic/fatty marrow. There were significant increases in the 2-week revascularization and the 4-week revascularization and new bone formation in the MR16-1 group compared to the saline group. Mann-Whitney *U* test was used between treatments. Values were expressed by a box plot. 2 weeks (saline; n = 7, MR16-1; n = 8), 4 weeks (saline; n = 13, MR16-1; n = 15), $^{**}p < 0.01$.

ischemic induction as seen in the saline treated ON side (Figs. 1 and 2). With MR16-1 therapy, bone volume and new bone formation were increased (Figs. 1–3), consistent with the results observed in the adolescent IL-6 KO mice following ischemic ON [9].

Previously we administered tocilizumab into immature 6-week-old mice following ischemic induction and found increased epiphyseal bone mass [10]. In the current study, we used adolescent 12-week-old mice as ON in adolescence is particularly challenging to treat. Adolescent JIO is known to have significantly worse clinical prognosis and outcome [3,4]. In adolescent mice we observed that the capability for new bone formation following ischemic ON was substantially lower than those of immature mice, based on our previous study [23]; the mean BFR and MAR were about 50~70% lower. In addition to using older mice, we used MR16-1 instead of tocilizumab in this study as MR16-1 was specifically developed for use in mice to inhibit IL-6 receptor while tocilizumab was developed for human IL-6 receptor inhibition. Despite these differences, the findings from the previous and current studies suggest that IL-6 receptor inhibition has beneficial effects on new bone formation in the context of JIO.

4.3. Effects of IL-6 receptor blockade on revascularization

In this study, we found that IL-6 receptor inhibition increased revascularization and replacement of the necrotic marrow with new hematopoietic bone marrow at 2- and 4-weeks following ischemic induction (Fig. 5). Based on these findings, we postulate that increased revascularization promotes hematopoietic stem cell recruitment and hematopoietic marrow niche formation. Furthermore, we postulate that early restoration of the hematopoietic marrow stimulates the differentiation of mesenchymal stem cells (MSC) and osteoprogenitor cells to osteoblasts [32]. Increased new bone formation may also be due to a direct effect of IL-6 blockade as pro-inflammatory cytokines including IL-6, IL-1β (i.e., an upstream activator of IL-6 [26]), and TNF-α, are known to inhibit osteogenic differentiation of mouse MSC [16,33].

Our recent study using a piglet model of JIO showed that macrophages in the repair tissue produced IL-6, IL-1β, and TNF-α following ischemic induction [34]. While macrophages have bone catabolic roles through pro-inflammatory cytokines, it is known that certain macrophage phenotype is associated with bone anabolism by releasing bone morphogenetic protein 2 (BMP-2), BMP-4, and transforming growth factor beta 1 (TGF-β1) [35,36]. More intriguingly, bone resident macrophages, termed osteal macrophages [37], have recently been classified as being distinct from osteoclasts, and shown to support osteoblast function in bone homeostasis and bone repair [38]. In the context of ischemic ON, however, the role of osteal macrophages is unknown. In animal models of JIO, we previously reported that IL-6 [8], BMP-2 [25], VEGF [39], and HIF-1α [40] are all increased following ischemic induction with accumulation of activated macrophages [41]. Because BMPs stimulate angiogenesis through the production of VEGF [42], and HIF1-α and VEGF regulate each other [43], the molecular mechanisms

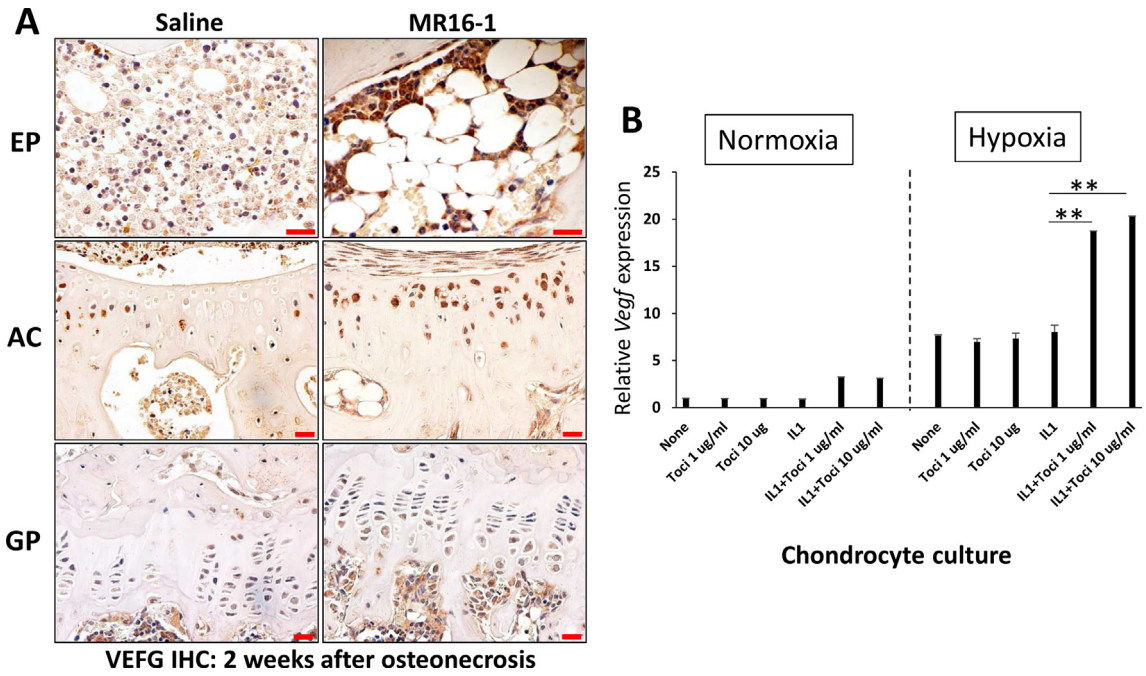

Fig. 6. The assessment of VEGF expression at 2 weeks post-surgery *in vivo* and under hypoxic chondrocyte culture *in vitro*. (A) VEGF immunohistochemistry (IHC) showed increased VEGF expression in the areas of revascularization in the necrotic epiphysis (EP) of the MR-16 group at 2 weeks compared to the saline group. VEGF expression was also increased in the articular cartilage (AC) of the MR16-1 group while it was unchanged in the growth plate cartilage (GP). Scale bar; 20 μm . (B) Human chondrocytes were pretreated with tocilizumab (1 μg/ml, 10 μg/ml) for 1 h, followed by IL1-β exposure under normoxia (20% oxygen) or hypoxia (1% oxygen) for 16 h. Expression levels of *VEGF* were significantly increased with tocilizumab pretreatment. The value of the non-treatment group (i.e., no treatment under normoxia) was set as 1.0. Kruskal-Wallis test followed by Mann-Whitney *U* test was used among 3 conditions with IL-1 treatment under hypoxia (IL-1, IL-1+1 μg/ml tocilizumab, and IL-1+10 μg/ml tocilizumab). Values were expressed by the mean ± SD. Note that relative *VEGF* expression levels in hypoxia were higher compared to those in normoxia. $^{**}p < 0.01$.

underlying increased revascularization and new bone formation following IL-6 receptor blockade in the context of ischemic ON and macrophage are of great interest for future studies.

We previously reported that chondrocytes in the articular cartilage are viable following ischemic induction and can express several molecules by responding to a hypoxic change *in vivo* including IL-6 [8], BMP2 [25], and VEGF [39]. In the adolescent IL-6 KO mice, VEGF expression and revascularization following ischemic ON were enhanced in the necrotic epiphyseal bone marrow space compared to wild-type control [9]. In the current study, we obtained similar results as VEGF was further increased when IL-6 receptor was blocked *in vitro* and *in vivo* (Fig. 6) and propose that the inhibition of IL-6 signaling enhances revascularization and bone formation through upregulation of VEGF and BMP [10] from articular chondrocytes, not from growth plate chondrocytes, in the context of ischemic ON (Fig. 7).

In the current study, we postulate that pro-angiogenic factor, VEGF, increased revascularization despite inhibition of IL-6 signaling due to compensatory mechanisms involving the activation of other angiogenic cytokines. In fact, other pro-angiogenic factors, such as IL-8 and TNF-α [44], were increased in cultured chondrocytes treated with IL-6 receptor blocker (Supple. Fig. 2). Future studies are needed to determine the mechanisms by which cartilage metabolism following ischemic ON contributes to revascularization through VEGF.

4.4. Effects of IL-6 receptor blockade on bone resorption

It has been reported that pro-inflammatory cytokines including IL-6 consistently up-regulate the expression of receptor activator of NF-κB ligand (RANKL) [45] which activates the master gene for osteoclastogenesis called nuclear factor of activated T cells cytoplasmic 1 (NFATc1) [45]. *In vitro* studies using mouse cells showed that IL-6 stimulates osteoclast formation [46] by promoting RANKL production from osteoblast lineage cells [15]. *In vivo* study using TNF-α transgenic mice showed that IL-6 receptor inhibition attenuated osteoclast formation in the inflammatory region [47].

In the current study, we did not observe a decrease in osteoclast number in adolescent mice following JIO with IL-6 receptor inhibition (Fig. 4). It is interesting to note that we observed significantly increased osteoclast numbers in adolescent IL-6 KO mice following ischemic induction in our previous study [9]. In addition, gain-of-function of IL-6 in the adolescent IL-6 transgenic mice did reduce osteoclast number and bone resorption [48] probably because IL-6 supports osteoclast formation in a RANKL independent mechanism [49]. In some conditions, IL-6 conversely inhibits osteoclast differentiation by suppressing RANK signaling pathways through MAPK using mouse cells *in vitro* [50]. Thus, it seems that IL-6 effects on osteoclasts and bone resorption are complex and not straightforward in a context-dependent manner (i.e., by age). Future studies are needed to investigate the paradoxical role of IL-6 in the bone catabolism.

4.5. Limitations of this study

This study has limitations. The distal femoral epiphysis was selected instead of the proximal epiphysis because of the differences in development. The distal epiphysis develops via the formation of a secondary ossification center, similar to the case in humans (i.e., human femoral head develops via a secondary ossification center). Conversely, the proximal epiphysis (i.e., femoral head) of the mouse develops by direct ossification of calcified cartilage via migration of metaphyseal blood vessels [51], requiring the interruption of blood supply from the metaphysis in addition to external vessels in order to induce ON. In addition, it is technically difficult to induce femoral head ON in mice without causing iatrogenic hip dislocation, femoral neck fracture, and/or extensive soft tissue damage due to the deep location of the bone [22].

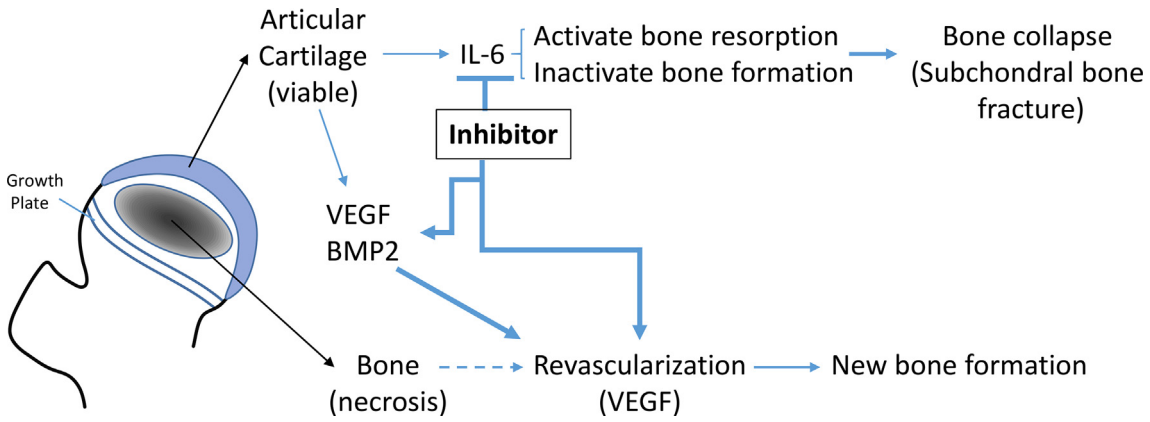

Fig. 7. A working model in which VEGF and BMP2 expressed by articular cartilage play an important role in revascularization and new bone formation following ischemic ON. IL-6 is largely produced by articular cartilage which is viable under hypoxic condition. IL-6 activates bone resorption and inactivate bone formation, resulting in bone collapse called subchondral bone fracture in the epiphysis. The onset of LCPD before six years of age is generally associated with a good outcome even without treatment, while age at onset after age nine, and especially in teenagers, is associated with worse outcome, probably because the revascularization in the necrotic bone is not enough. The inhibition of IL-6 signaling can restrain bone collapse by increasing bone volume and enhance revascularization directly or indirectly through upregulation of bone anabolic molecules, VEGF and BMP2, from articular cartilage, leading to new bone formation.

5. Conclusions

In conclusion, our findings indicate that IL-6 receptor blockade in adolescent mice following JIO increases revascularization and new bone formation. The findings suggest IL-6 receptor blocker as a potential medical therapy for adolescent JIO.

Contributions

Authors' roles: GK, NK, and HK designed experiments, reviewed data. GK and NK wrote the manuscript edited by HK. GK and RY performed the experiments and gathered data. All authors have read and approved the submitted manuscript.

Funding

This work was supported by funding from Scottish Rite for Children (H.K.) and JPJS KAKENHI (N.K. 15K08437, 19K09563, 23K08663, G.K. 17H07009, 19K18471).

Declaration of competing interest

The author (H.K.) has received tocilizumab from Genentech Inc. for an unrelated research work. All other authors have no conflicts of interest (COI). Study data will be available upon request without COI.

Acknowledgements

MR16-1 was kindly provided from Genentech Inc. for this research. Reuel Cornelia and Richard Banlaygas for histological preparation, Dr. Satoshi Hattori for advice on statistical analysis, and Elena Chen, Michael Kutschke, Naga Suresh Adapala, Olumide Aruwajoye, and Ila Oxendine for technical assistance.

Appendix A. Supplementary data

Supplementary data to this article can be found online at https://doi.org/10.1016/j.ocarto.2023.100386.

References

[1] J.A. Herring, H.T. Kim, R. Browne, Legg-Calve-Perthes disease. Part II: prospective multicenter study of the effect of treatment on outcome, J Bone Joint Surg Am 86-A (10) (2004) 2121–2134.
[2] S.B. Rosenfeld, J.A. Herring, J.C. Chao, Legg-calve-perthes disease: a review of cases with onset before six years of age, J Bone Joint Surg Am 89 (12) (2007) 2712–2722.
[3] B. Joseph, K. Mulpuri, G. Varghese, Perthes' disease in the adolescent, J Bone Joint Surg Br 83 (5) (2001) 715–720.
[4] E. Ippolito, C. Tudisco, P. Farsetti, Long-term prognosis of Legg-Calve-Perthes disease developing during adolescence, J. Pediatr. Orthop. 5 (6) (1985) 652–656.
[5] H.K. Kim, J.A. Herring, Pathophysiology, classifications, and natural history of Perthes disease, Orthop. Clin. N. Am. 42 (3) (2011) 285–295.
[6] H.K. Kim, Pathophysiology and new strategies for the treatment of Legg-Calve-Perthes disease, J Bone Joint Surg Am 94 (7) (2012) 659–669.
[7] N. Kamiya, et al., Legg-Calve-Perthes disease produces chronic hip synovitis and elevation of interleukin-6 in the synovial fluid, J. Bone Miner. Res. 30 (6) (2015) 1009–1013.
[8] R. Yamaguchi, et al., HIF-1-Dependent IL-6 activation in articular chondrocytes initiating synovitis in femoral head ischemic osteonecrosis, J Bone Joint Surg Am 98 (13) (2016) 1122–1131.
[9] G. Kuroyanagi, et al., Interleukin-6 deletion stimulates revascularization and new bone formation following ischemic osteonecrosis in a murine model, Bone 116 (2018) 221–231.
[10] N. Kamiya, et al., IL6 receptor blockade preserves articular cartilage and increases bone volume following ischemic osteonecrosis in immature mice, Osteoarthritis Cartilage 27 (2) (2019) 326–335.
[11] Y. Ren, et al., Anti-Interleukin-6 therapy decreases hip synovitis and bone resorption and increases bone formation following ischemic osteonecrosis of the femoral head, J. Bone Miner. Res. 36 (2) (2021) 357–368.
[12] S. Rose-John, et al., Targeting IL-6 trans-signalling: past, present and future prospects, Nat. Rev. Immunol. (2023) 1–16.
[13] M. Okazaki, et al., Characterization of anti-mouse interleukin-6 receptor antibody, Immunol. Lett. 84 (3) (2002) 231–240.
[14] L. Lazzaro, et al., IL-6 trans-signalling mediates trabecular, but not cortical, bone loss after ovariectomy, Bone 112 (2018) 120–127.
[15] N. Udagawa, et al., Interleukin (IL)-6 induction of osteoclast differentiation depends on IL-6 receptors expressed on osteoblastic cells but not on osteoclast progenitors, J. Exp. Med. 182 (5) (1995) 1461–1468.
[16] S. Kaneshiro, et al., IL-6 negatively regulates osteoblast differentiation through the SHP2/MEK2 and SHP2/Akt2 pathways in vitro, J. Bone Miner. Metabol. 32 (4) (2014) 378–392.
[17] F. De Benedetti, et al., Impaired skeletal development in interleukin-6-transgenic mice: a model for the impact of chronic inflammation on the growing skeletal system, Arthritis Rheum. 54 (11) (2006) 3551–3563.
[18] M.H. Hartman, et al., Inhibition of interleukin-6 receptor in a murine model of myocardial ischemia-reperfusion, PLoS One 11 (12) (2016) e0167195.
[19] V.L. Ferguson, et al., Bone development and age-related bone loss in male C57BL/6J mice, Bone 33 (3) (2003) 387–398.
[20] R. Voide, G.H. van Lenthe, R. Muller, Differential effects of bone structural and material properties on bone competence in C57BL/6 and C3H/He inbred strains of mice, Calcif. Tissue Int. 83 (1) (2008) 61–69.
[21] J.M. Somerville, et al., Growth of C57BL/6 mice and the material and mechanical properties of cortical bone from the tibia, Calcif. Tissue Int. 74 (5) (2004) 469–475.
[22] N. Kamiya, et al., Development of a mouse model of ischemic osteonecrosis, Clin. Orthop. Relat. Res. 473 (4) (2015) 1486–1498.
[23] R. Yamaguchi, et al., Development of a murine model of ischemic osteonecrosis to study the effects of aging on bone repair, J. Orthop. Res. 39 (12) (2021) 2663–2670.
[24] H.K. Kim, et al., Ibandronate for prevention of femoral head deformity after ischemic necrosis of the capital femoral epiphysis in immature pigs, J Bone Joint Surg Am 87 (3) (2005) 550–557.

[25] N. Kamiya, et al., Acute BMP2 upregulation following induction of ischemic osteonecrosis in immature femoral head, Bone 53 (1) (2013) 239–247.
[26] C.M. Cahill, J.T. Rogers, Interleukin (IL) 1beta induction of IL-6 is mediated by a novel phosphatidylinositol 3-kinase-dependent AKT/IkappaB kinase alpha pathway targeting activator protein-1, J. Biol. Chem. 283 (38) (2008) 25900–25912.
[27] K.J. Livak, T.D. Schmittgen, Analysis of relative gene expression data using real-time quantitative PCR and the 2(-Delta Delta C(T)) Method, Methods 25 (4) (2001) 402–408.
[28] J. Cohen, Statistical Power Analysis for the Behavioral Sciences, second ed., Lawrence Erlbaum, 1988, pp. 20–26.
[29] N. Franchimont, S. Wertz, M. Malaise, Interleukin-6: an osteotropic factor influencing bone formation? Bone 37 (5) (2005) 601–606.
[30] N.A. Sims, Cell-specific paracrine actions of IL-6 family cytokines from bone, marrow and muscle that control bone formation and resorption, Int. J. Biochem. Cell Biol. 79 (2016) 14–23.
[31] V. Poli, et al., Interleukin-6 deficient mice are protected from bone loss caused by estrogen depletion, EMBO J. 13 (5) (1994) 1189–1196.
[32] S.J. Morrison, D.T. Scadden, The bone marrow niche for haematopoietic stem cells, Nature 505 (7483) (2014) 327–334.
[33] D.C. Lacey, et al., Proinflammatory cytokines inhibit osteogenic differentiation from stem cells: implications for bone repair during inflammation, Osteoarthritis Cartilage 17 (6) (2009) 735–742.
[34] N.S. Adapala, et al., Necrotic bone stimulates proinflammatory responses in macrophages through the activation of toll-like receptor 4, Am. J. Pathol. 186 (11) (2016) 2987–2999.
[35] C.M. Champagne, et al., Macrophage cell lines produce osteoinductive signals that include bone morphogenetic protein-2, Bone 30 (1) (2002) 26–31.
[36] O. Fromigue, P.J. Marie, A. Lomri, Bone morphogenetic protein-2 and transforming growth factor-beta2 interact to modulate human bone marrow stromal cell proliferation and differentiation, J. Cell. Biochem. 68 (4) (1998) 411–426.
[37] B.P. Sinder, A.R. Pettit, L.K. McCauley, Macrophages: their emerging roles in bone, J. Bone Miner. Res. 30 (12) (2015) 2140–2149.
[38] L. Vi, et al., Macrophages promote osteoblastic differentiation in-vivo: implications in fracture repair and bone homeostasis, J. Bone Miner. Res. 30 (6) (2015) 1090–1102.
[39] H.K. Kim, et al., Increased VEGF expression in the epiphyseal cartilage after ischemic necrosis of the capital femoral epiphysis, J. Bone Miner. Res. 19 (12) (2004) 2041–2048.
[40] H.K. Kim, et al., Hypoxia and HIF-1alpha expression in the epiphyseal cartilage following ischemic injury to the immature femoral head, Bone 45 (2) (2009) 280–288.
[41] M.C. Phipps, et al., In vivo monitoring of activated macrophages and neutrophils in response to ischemic osteonecrosis in a mouse model, J. Orthop. Res. 34 (2) (2016) 307–313.
[42] M.M. Deckers, et al., Bone morphogenetic proteins stimulate angiogenesis through osteoblast-derived vascular endothelial growth factor A, Endocrinology 143 (4) (2002) 1545–1553.
[43] J.J. Deudero, et al., Induction of hypoxia-inducible factor 1alpha gene expression by vascular endothelial growth factor, J. Biol. Chem. 283 (17) (2008) 11435–11444.
[44] R. Heidenreich, M. Rocken, K. Ghoreschi, Angiogenesis drives psoriasis pathogenesis, Int. J. Exp. Pathol. 90 (3) (2009) 232–248.
[45] H. Takayanagi, Osteoimmunology: shared mechanisms and crosstalk between the immune and bone systems, Nat. Rev. Immunol. 7 (4) (2007) 292–304.
[46] T. Tamura, et al., Soluble interleukin-6 receptor triggers osteoclast formation by interleukin 6, Proc. Natl. Acad. Sci. U. S. A. 90 (24) (1993) 11924–11928.
[47] R. Axmann, et al., Inhibition of interleukin-6 receptor directly blocks osteoclast formation in vitro and in vivo, Arthritis Rheum. 60 (9) (2009) 2747–2756.
[48] H. Kitamura, et al., Bone marrow neutrophilia and suppressed bone turnover in human interleukin-6 transgenic mice. A cellular relationship among hematopoietic cells, osteoblasts, and osteoclasts mediated by stromal cells in bone marrow, Am. J. Pathol. 147 (6) (1995) 1682–1692.
[49] O. Kudo, et al., Interleukin-6 and interleukin-11 support human osteoclast formation by a RANKL-independent mechanism, Bone 32 (1) (2003) 1–7.
[50] F. Yoshitake, et al., Interleukin-6 directly inhibits osteoclast differentiation by suppressing receptor activator of NF-kappaB signaling pathways, J. Biol. Chem. 283 (17) (2008) 11535–11540.
[51] H.A. Cole, et al., Differential development of the distal and proximal femoral epiphysis and physis in mice, Bone 52 (1) (2013) 337–346.